

Buckling of Si and Ge (111)2×1 Surfaces

Shu Nie and R. M. Feenstra

Dept. Physics, Carnegie Mellon University, Pittsburgh, PA 15213, USA

Ji Young Lee and Myung-Ho Kang

Dept. Physics, Pohang University of Science and Technology, Pohang 790-784, Korea

Voltage-dependent scanning tunneling microscopy is used to determine the buckling of π -bonded chains on Si and Ge(111)2×1 surfaces. Images are acquired over a wide range of voltages, and are compared with theoretical constant-density contours generated from first-principles electronic-structure calculations. The theoretical predictions for $\langle 2\bar{1}\bar{1} \rangle$ corrugation shifts are quite different for positive and negative buckling; experimental results for Si are found to agree with the former and those for Ge agree with the latter. In addition to an expected shift in $\langle 2\bar{1}\bar{1} \rangle$ corrugation between small-magnitude positive and negative voltages, a further shift is also seen in both experiment and theory between small and large positive voltages.

I. Introduction

The 2×1 reconstructions of Ge(111) and Si(111) surfaces have served as prototypical systems for the investigation of surfaces electronic and optical properties. It is well accepted that the geometry of the surfaces is described by the π -bonded chain model [1]. Buckled chain configurations are favored energetically, but it was found to be difficult to theoretically predict the buckling direction of the chains since two possible buckling directions appear quite similar both in energetics and in surface band structures [2]. Nevertheless, Rohlfing et al. [3], following the work of Takeuchi et al. [4], has proposed that the Si and Ge surface might have opposite buckling, based on a comparison of theoretical bandgaps with experimental results from photoemission and inverse photoemission spectroscopy as well as a comparison of computed optical spectra with experimental data. Conclusive determination of the buckling for each surface is important, to enable further use of these surface as prototypes for investigation of new experimental and theoretical techniques.

In previous works we have investigated the buckling of these surfaces using scanning tunneling microscopy (STM) [5,6]. STM provides a relatively direct means of determining surface buckling (at least for large buckling), as illustrated in Fig. 1. In the somewhat oversimplified view illustrated there, large buckling produces upper and lower atoms in the chains, with filled states being localized on the upper atoms and empty states on the lower ones. Thus, observation of the relative position (i.e. corrugation shift) between filled and empty states of a chain then directly yields the sense (so-called "positive" or "negative") of the buckling. Early STM works investigating Si(111)2×1 did indeed observe a positive $\langle 2\bar{1}\bar{1} \rangle$ corrugation shift of empty states relative to filled ones, consistent with positive buckling [2,5]. However, the voltage dependence of the corrugation shift was not examined in detail, and also, a later careful examination of results from an extended set of experiments produced some uncertainty in the sign of this

corrugation shift [7]. STM studies on the Ge(111) surface produced a shift of empty states relative to filled ones in the $\langle \bar{2}11 \rangle$ direction [6], i.e. consistent with negative buckling for that surface. In the present work, we extend our STM measurements to include both Si(111) and Ge(111) surfaces, with all measurements performed using the same STM and with identical sample geometry so that no confusion over the relative identification $\langle 2\bar{1}\bar{1} \rangle$ vs. $\langle \bar{2}11 \rangle$ surface directions can arise. STM images are acquired at many voltages ranging from -2 V to $+2$ V, and then compared with theoretical STM images simulated from density-functional theory calculations. The theory reveals that the corrugation shift between filled and empty states *does* follow the simple expectation shown in Fig. 1 for voltages with small magnitude, but at larger positive voltages the corrugation shift further evolves due to the nonzero amplitude of the surface electronic wavefunctions on *both* atoms in the unit cell. From a comparison between theory and experiment, it is conclusively demonstrated that the Ge(111) 2×1 surface is negatively buckled and the Si(111) 2×1 surface is positively buckled.

II. Experimental

Pieces of $\{111\}$ oriented Si and Ge wafers, both *n*-type with resistivities of 0.002 and 0.2 Ω -cm, respectively, were cleaved in ultrahigh vacuum to expose a (111) face. The geometry of the cleaving and sample holder is identical to that described in our previous work [6], whereas the scanning direction for the room-temperature STM used here is opposite of that used in Ref. [6]. The STM employed for this work is routinely used for cross-sectional measurements of semiconductor heterostructures, so that the scanning directions are definitively known. Thus, the distinction between $\langle 2\bar{1}\bar{1} \rangle$ and $\langle \bar{2}11 \rangle$ directions in our images can be made with complete certainty. Images were acquired with a constant current of 0.1 nA. Voltage-dependent imaging was performed using the technique of varying the voltage on a line-by-line basis such that very little drift occurs between the images of a set (a small drift correction is applied to the entire set to achieve the known dimensions of the 2×1 unit cell, and in this way the relative position of the images within the set is determined without any further adjustment). Commercially available Pt-Ir probe tips were used, and they were cleaned *in situ* using electron bombardment.

III. Results

Figure 2 shows typical voltage-dependent images, in this case for the Ge(111) surface. The π -bonded chains are apparent, with a single corrugation maximum per 2×1 unit cell. In Fig. 2 the $\langle 01\bar{1} \rangle$ corrugation (i.e. *along* the chains) is better defined at negative compared to positive voltages, and this is a general feature of all of our data acquired from both Si and Ge surfaces. Data such as that shown in Fig 2 is analyzed by fitting the images to a function consisting of the sum of two sinusoids extending in perpendicular directions and with adjustable phase and amplitudes. The wavevectors for the sinusoids are determined from the dimensions of the unit cell, and are identical for all images within a set. The phase of the $\langle 2\bar{1}\bar{1} \rangle$ -directed sinusoid then gives the corrugation shift

(with arbitrary zero) for that particular voltage. It is these $\langle 2\bar{1}\bar{1} \rangle$ corrugation shifts which provide us with information on the buckling of the chains.

Our experimental results for the $\langle 2\bar{1}\bar{1} \rangle$ corrugation shifts are summarized in Fig 3. We plot data from four separate experiments for Si and three Ge, with each experiment performed using a separate probe tip. The absolute zero for the corrugation shift within each set is arbitrary, and the results from different sets are aligned such that they approximately overlap. The reproducibility of the results between different experiments is quite good. For empty states (positive sample voltages) the shifts for Ge reveal a monotonically increasing behavior, with relatively large slope, whereas for Si we find a monotonically decreasing behavior, again with relatively large slope. The results for filled states show somewhat more variability for different experiments, but an overall trend of a corrugation which is relatively constant (for Ge) or increases gradually with increasing voltage-magnitude (for Si), is suggested by an average of the data sets for each material.

We have performed six experiments each for Ge(111) and Si(111) surfaces. Within a given experiment, detailed voltage-dependent results such as those shown in Fig. 3 are measured generally at 3 or 4 different locations over the surface. Thus, in total we have acquired and analyzed 32 data sets for Ge and 16 for Si. We find that *all* of the data sets for Ge show good reproducibility (with the results of Fig. 3 being typical of the set), whereas for Si, data from 5 out of 6 of the experiments show good reproducibility and that from the remaining experiment shows significantly different results. We exclude data from that single experiment from consideration, and we tentatively attribute those results to an anomalous (nonmetallic) probe-tip. Theoretically predicted corrugation shifts are also included in Fig. 3 and will be discussed in detail in Section IV.

We also comment on the reproducibility of the buckling results at differing surface locations. It has been suggested previously [8], for the case of Ge in particular, but some surface areas may be buckled differently than others (i.e. two nearly equivalent energy minima may exist for the buckling, one for positive and the other for negative buckling). To investigate this possibility we have performed imaging of the surface over a larger scale than that shown in Fig 2. As described in Section IV, the most reliable and sensitive means of determining buckling is *not* to compare images at positive and negative voltage, but rather, to examine images at differing small-magnitude positive voltages (as seen in Fig. 3, the corrugation shifts vary quite rapidly at small positive voltages, with a sense of this variation in opposite for positive and negative bucklings). Hence, we acquired images at voltages of typically +1.0 and +1.4 V, with typical results shown in Figs. 4(a) and (b), respectively. In this case, for Ge, the images display both 2×1 domains and areas covered with Ge adatoms, as previously described [9]. Also, a domain boundary between different 2×1 domains is apparent in the images. The inset in each image shows an expanded view of the corrugation, and a fixed location on the surface is marked in each inset. The $\langle 2\bar{1}\bar{1} \rangle$ corrugation shift between the data of Fig. 4(a) and (b) is not readily apparent from the respective images, but it can easily be determined from our fitting procedure described above (we find a value of $20\pm 7^\circ$ in this case). Acquisition of these large-scale images has been repeated at many locations (>20 for Ge and >10 for Si) on multi-domain 2×1 surfaces of each material, and in both cases we find a single, unique

result for the sense of the buckling at all surface locations. We thus conclude that, although buckling may change near surface defects and/or domain boundaries, we find no evidence of surface domains (for a given material) having different buckling.

IV. Discussion

To determine the buckling of the π -bonded chains based on the STM data one can, to lowest order, use the argument presented in Fig. 1. However, it is clear that this argument is oversimplified, since it fails to take into account the complete dispersion relationship of the surface states. It is well known from a simple two-inequivalent-atom model of the surface band structure that the states which lie near the band edges do indeed have character as pictured in Fig. 1 (with zero occupation on one atom or the other of the chain), but as one moves further into the bands then the wavefunction acquires nonzero amplitude on both atoms of the chain through a coupling between the filled and empty dangling-bond states [10]. Thus, a better way of understanding the STM images is to examine theoretical STM images over a range of sample-tip voltages for given buckling, and then to compare the resulting corrugation shifts with the experiment.

We have performed pseudopotential density-functional calculations within the generalized gradient approximation [11]. In order to accurately determine the corrugation shifts, we employed a ten-layer slab geometry with H termination, a plane-wave basis of 15 Ry, and a (2×1) Brillouin-zone sampling of uniform 32 \mathbf{k} -points, which are better computational parameters than those used in our previous studies [2,11]. The present calculations produce positive (negative) bucklings of 0.52 Å (0.59 Å) for Si and 0.80 Å (0.83 Å) for Ge, in good agreement with the positive bucklings of 0.51 Å for Si and 0.84 Å for Ge calculated by Rohlfing et al. [3,12]. The energy differences between the positive and negative bucklings for both Si and Ge are all negligible to within 0.005 eV/surface-atom.

Typical theoretical STM images are shown in Fig. 5, showing negatively buckled Ge(111) 2×1 . For voltages with low magnitude (Figs. 5(a) and (b)), we see the empty state-density is localized on the lower atom of each unit cell and the filled state-density on the upper atom, consistent with the simple picture of Fig. 1. However, as the voltage increases, additional effects occur due to the nature of the surface band dispersion mentioned before. In particular, for empty states, as the voltage increases the upper atom starts to appear, and at a relatively large voltage of +1.25 V (Fig. 5(f)), it dominates the image. This behavior occurs because even though the wavefunction on this atom may have a somewhat smaller amplitude, its higher position means that it appears in the images more prominently than the lower atom. In contrast, for the filled states, the wavefunction for low-magnitude voltages is localized primarily on the upper atom, so that as the voltage increases in magnitude it is this same atom which dominates the images. This behavior is consistent with the observed nature of our images, Fig. 2, in which we reproducibly find a relatively large $\langle 01\bar{1} \rangle$ corrugation for the filled states, but a much smaller one for the empty states.

Theoretical results for corrugation shifts are obtained from the simulated STM images. We place the origin of our coordinate system on the upper atom of the unit cell, and then locate the brightest position in the simulated images. The $\langle 2\bar{1}\bar{1} \rangle$ component of this position is plotted in Fig. 3, together with the experimental data. We include in Fig. 3 the

theoretical results which most closely agree with the experimental data, namely, the positively buckled results for Si, and the negatively buckled results for Ge. There is relatively little difference between the results for Si and Ge, and also, the results for positive and negative buckling are given nearly by the negative of each other. An examination of Fig. 3 reveals that the theoretical results are indeed consistent with the experiments, whereas interchanging the theoretical results between Figs. 3(a) and (b) would produce inconsistency between experiment and theory. We note that the discontinuous nature of the theoretical results at small voltages of 0.5–1.0 V arises from the shift in location of intensity-maxima of the simulated images between the lower and upper atoms as described above. In contrast, for the experimental results, this shift appears smeared out over a finite voltage range because the nature of the sinusoidal fitting procedure (used to extract the phase shifts) weights both atoms in the unit cell.

Comparing the present experimental results with past ones, we find the same sign for the corrugation shift as seen in the prior Ge(111) work [6], and also the same sign as deduced from some of the early Si(111) work [2,5]. These conclusions are nontrivial ones however, since, as revealed by the present study, the sign of the corrugation shift can change depending on the magnitude of the positive voltage used. In general, in the past work, voltages with the minimum possible magnitude (compatible with stable STM imaging) were used. It is clear that this choice is the appropriate one to ensure the applicability of the simple interpretation of the data, *i.e.* as in Fig. 1. Nevertheless, as demonstrated here, the range of applicability of this simple interpretation is really quite narrow, and experimentally one must use *very* small voltages to ensure a correct interpretation. (It is possible that the inconsistency found during our re-analysis of an extended set of the Si(111) results [7] in the sign of the corrugation shift resulted from unintentional use of positive voltages which were too high). A more reliable scheme, as used in the present work, is to acquire data over a larger range of voltages and then make the comparison with simulated STM images.

V. Summary

In summary, we have used voltage-dependent STM imaging in conjunction with first-principles theoretical calculations to determine unambiguously the sign of the buckling for Si(111) and Ge(111) 2×1 surfaces. We find positive buckling for Si, and negative buckling for Ge. The interpretation of the voltage-dependent images in terms of revealing simply the upper atoms in filled states and the lower atoms in empty states is shown to be valid only for very low sample-tip voltages. At higher, positive voltages, the images undergo another reversal, with the upper atoms dominating.

Acknowledgements

This work has been supported by the U.S. National Science Foundation, grant DMR-9985898. MHK acknowledges support from the Korea Science and Engineering Foundation through the ASSRC at Yonsei University.

References:

1. K. C. Pandey, Phys. Rev. Lett. **47**, 1913 (1981); **49**, 223 (1982).
2. S.-H. Lee and M.-H. Kang, Phys. Rev. B **54**, 1482 (1996); *erratum* Phys. Rev. B **55**, 1903 (1997).
3. M. Rohlfing, M. Palumbo, G. Onida, and R. Del Sole, Phys. Rev. Lett. **85**, 5440 (2000).
4. N. Takeuchi, A. Selloni, A. I. Shkrebtii, and E. Tosatti, Phys. Rev. B **44**, 13611 (1991).
5. J. A. Stroschio, R. M. Feenstra, and A. P. Fein, Phys. Rev. Lett. **57**, 2579 (1986).
6. R. M. Feenstra, G. Meyer, F. Moresco, and K. H. Rieder, Phys. Rev. B **64**, 081306 (2001).
7. R. M. Feenstra (unpublished).
8. H. Hirayama, N. Sugihara, and K. Takanayagi, Phys. Rev. B **62**, 6900 (2000).
9. R. M. Feenstra, Phys. Rev. B **44**, 13791 (1991).
10. R. Del Sole and A. Selloni, Phys. Rev. B **30**, 883 (1984).
11. J. Y. Lee and M.-H. Kang, Phys. Rev. B **66**, 233301 (2002), and references therein.
12. M. Rohlfing and S. G. Louie, Phys. Rev. Lett. **83**, 856 (1999).

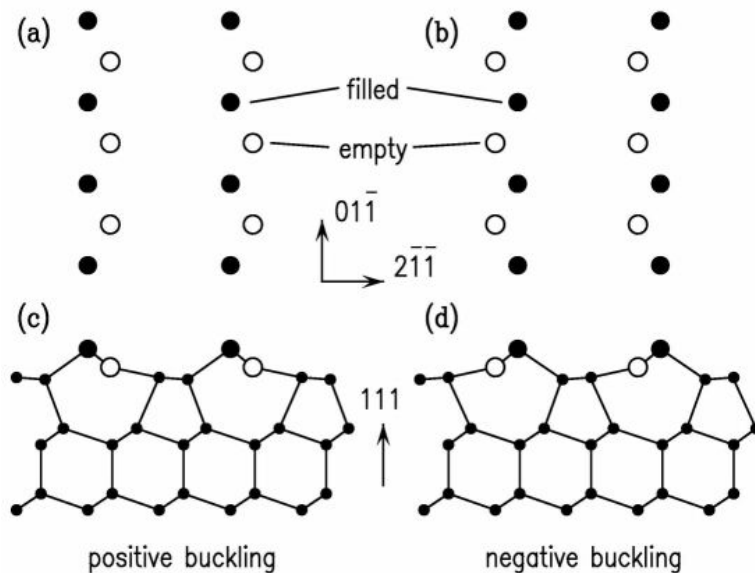


FIG. 1. Structural models for positively buckled [(a) and (c)] and negatively buckled [(b) and (d)] π -bonded chains, following Rohlfing *et al.* (Ref. [3]). A side view of the structures is shown in (c) and (d), and a top view of the atoms in the chains is shown in (a) and (b). Surface atoms whose dangling bonds are mainly filled (empty) of electrons are marked by solid (open) circles.

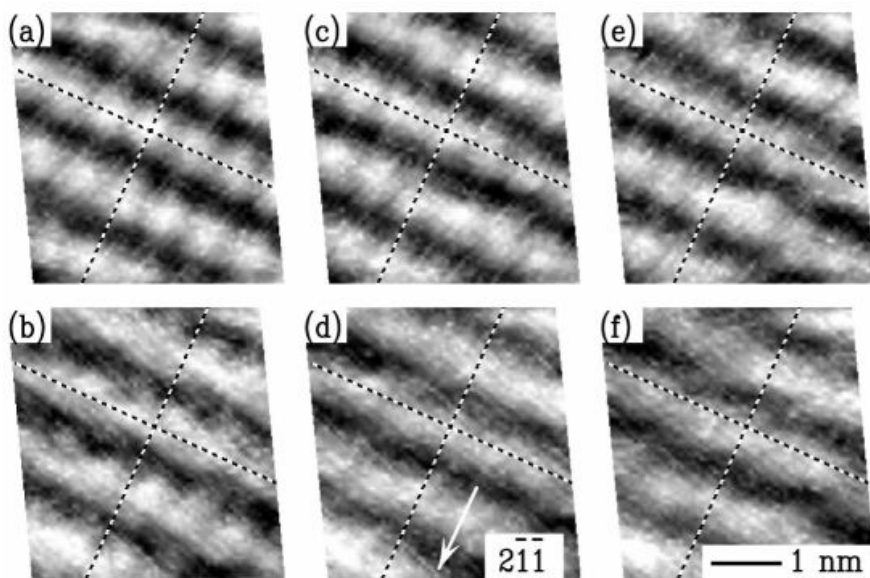


FIG. 2. STM images of the Ge(111) 2×1 surface, acquired at sample voltages of (a) -0.8 , (b) $+0.8$, (c) -1.3 , (d) $+1.3$, (e) -1.9 , and (f) $+1.9$ V. Dashed lines indicate the same surface locations in each image. Gray scale ranges are in the range $0.4\text{--}0.6$ Å.

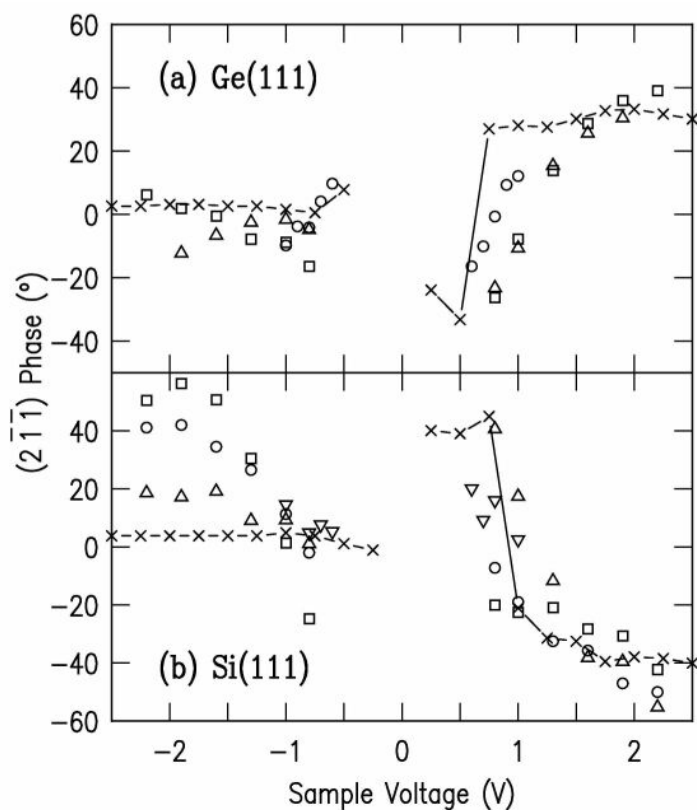


FIG. 3. $\langle 2\bar{1}\bar{1} \rangle$ corrugation phase shifts, for the experiments (open symbols) and theory (\times -marks). Theoretical results are shown for positive buckling for Si and negative buckling for Ge. The $\langle 2\bar{1}\bar{1} \rangle$ corrugation is measured relative to the upper atom of the chain in the case of the theory. The absolute zero of the corrugation phase is not known for the experiment, and the experimental data sets are shifted to approximately align them with the theoretical results.

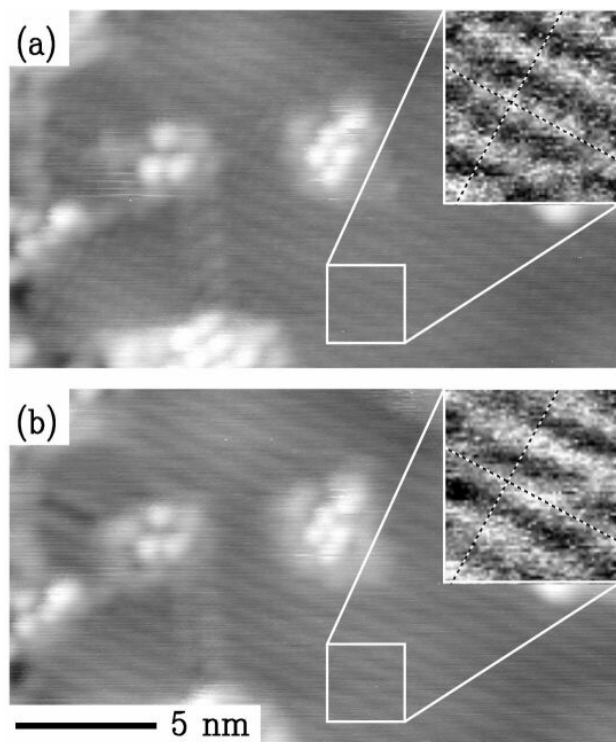


FIG. 4. Large-scale STM image of the Ge(111)2 \times 1 surface, acquired at sample voltages of (a) +1.0 and (b) +1.4 V. An inset in each image, at identical surface locations in (a) and (b), shows an expanded view of the surface with a fixed surface location marked. Gray scale range is 3 Å for both large images, and 0.3 Å for both insets.

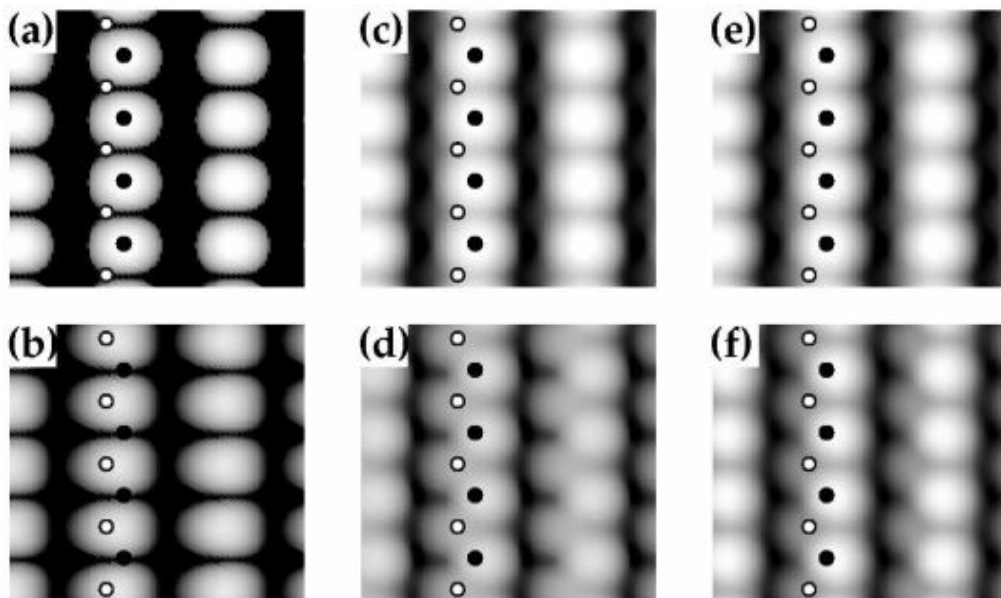


FIG. 5. Simulated constant-density STM images of the Ge(111)2 \times 1 surface with negative buckling at sample voltages of (a) -0.5, (b) +0.25, (c) -1.0, (d) +0.75, (e) -1.5, and (f) +1.25 V. The upper (lower) atoms in each unit cell are shown by solid (open) circles. The images were obtained by integrating the local density of states from the Fermi level to the given sample voltages. All the images represent the surface of a constant density of $7 \times 10^{-5} e/\text{Å}^3$.